Supplemental Material for "Three-phase Majorana zero modes at tiny magnetic fields"

Omri Lesser,[1,*] Karsten Flensberg,[2] Felix von Oppen,[3] and Yuval Oreg[1]

[1]Department of Condensed Matter Physics, Weizmann Institute of Science, Rehovot, Israel 7610001
[2]Center for Quantum Devices, Niels Bohr Institute, University of Copenhagen, DK-2100 Copenhagen, Denmark
[3]Dahlem Center for Complex Quantum Systems and Fachbereich Physik, Freie Universität Berlin, Arnimallee 14, 14195 Berlin, Germany

RELATION BETWEEN f AND WINDING

Here we prove the relation between $f(\phi_1, \phi_2, \phi_3)$, that appears in Eq. (2) of the main text, and phase winding. Without loss of generality, let us set $\phi_3 = 0$ and $\phi_2 > \phi_1$, and examine

$$f(\phi_1, \phi_2, 0) = \cos(\phi_1) + \cos(\phi_2) + \cos(\phi_2 - \phi_1). \quad \text{(S1)}$$

It is instructive to factor this expression using trigonometric identities:

$$\begin{aligned} f(\phi_1, \phi_2, 0) &= 2\cos\left(\frac{\phi_1+\phi_2}{2}\right)\cos\left(\frac{\phi_2-\phi_1}{2}\right) + 2\cos^2\left(\frac{\phi_2-\phi_1}{2}\right) - 1 \\ &= 2\cos\left(\frac{\phi_2-\phi_1}{2}\right)\left[\cos\left(\frac{\phi_1+\phi_1}{2}\right) + \cos\left(\frac{\phi_2-\phi_1}{2}\right)\right] - 1 \\ &= 4\cos\left(\frac{\phi_2-\phi_1}{2}\right)\cos\left(\frac{\phi_1}{2}\right)\cos\left(\frac{\phi_2}{2}\right) - 1. \end{aligned} \quad \text{(S2)}$$

The phases wind, i.e., the triangle connecting them encircles the origin, if and only if

$$0 \le \phi_1 \le \pi, \quad \pi \le \phi_2 \le \pi + \phi_1. \quad \text{(S3)}$$

It follows that

$$\cos\left(\frac{\phi_1}{2}\right) > 0, \cos\left(\frac{\phi_2}{2}\right) < 0, \cos\left(\frac{\phi_2-\phi_1}{2}\right) > 0. \quad \text{(S4)}$$

Therefore, the first term in Eq. (S2) is non-positive, and thus $f \le -1$. In addition, it is straightforward to show that along the boundaries defined by Eq. (S3), $f = -1$ exactly, and that $f(\phi_1, \phi_2, 0)$ has extrema only at the points $(\phi_1, \phi_2) = \left(\frac{2\pi}{3}, \frac{4\pi}{3}\right), (0, \pi), (\pi, \pi), (\pi, 2\pi)$. This concludes the proof that phase winding occurs if and only if $f \le -1$.

FURTHER ANALYSIS OF THE PHASE DIAGRAM

In this section we provide further details of the phase diagram in the coupled-wires model. The derivations are based on Eq. (2) of the main text, which determines the phase boundaries.

We begin by setting $t_\perp = 1$, and writing the solution of Eq. (2) which is a quadratic equation for Λ:

$$\Lambda_\pm = \frac{1}{2}\left[\mu\left(\Delta^2 f + 3 - \mu^2\right) \pm |\Delta| \sqrt{\mu^2\left[f\left(\Delta^2 f + 4\right) + 6 - 3\Delta^2\right] - \left[\Delta^2(\Delta^2 + 2f) + (2f+3)\left(1+\mu^4\right)\right]}\right]. \quad \text{(S5)}$$

In order to have a real solution, the argument of the square root must be non-negative. Treating the argument of the square root as a second-order polynomial in μ^2, we find that the condition for a real solution is

$$(f-3)(f+1)\left(\Delta^2(f+1)^2 + 8f + 12\right) \ge 0. \quad \text{(S6)}$$

Since $-3/2 \le f \le 3$, the first factor is negative whereas the last factor is positive. Therefore, this inequality is fulfilled only when $f \le -1$. This result, combined with our previous proof that $f \le -1$ corresponds to phase winding, is in agreement with Ref. [1].

The manifold in μ, Δ, Λ parameter space defined by Eq. (S5) is shown in Fig. S1 for several values of f. As explained in the main text, the parameters μ, Δ, Λ are said to be "optimal" if they support a solution of Eq. (2) for $f = -1$, i.e., if the necessary condition $f \le -1$ is also sufficient. Solving again for Λ, we obtain

$$\Lambda_\pm = \frac{1}{2}\left[\mu\left(3 - \Delta^2 - \mu^2\right) \pm \sqrt{-\Delta^2\left(1 - \Delta^2 - \mu^2\right)^2}\right]. \tag{S7}$$

The only way to make this expression real is demanding $\mu^2 + \Delta^2 = 1$. In this case the two solutions $\Lambda_\pm$ are identical and equal to $\mu/t_\perp$. This gives us the optimal curve $\mathcal{C}$ – the circle $\left(\mu, \sqrt{1-\mu^2}, \mu\right)$.

It is worth noting that along this circle, one can make a simple connection to the continuum description, thus finding an optimal condition for topological superconductivity in experimental system parameters. If we take $\Delta/t_\perp$ to be small (which means $\mu \approx t_\perp$), we obtain $\lambda \approx \Delta/t_\perp$ (assuming $\lambda_1 = \lambda_2 = \lambda_3 = \lambda$). In our minimal three-wires tight-binding description, the effective lattice spacing is the typical distance between two superconductors W. Using a continuum description of the tight-binding model along the circumference, we get $\Delta_{\rm SO} \approx t_\perp \lambda^2$. Since λ is the spin-dependent angle accumulated when hopping between nearest neighbors, and $\ell_{\rm SO}$ is the distance where a phase of 2π is accumulated, we have $W/\ell_{\rm SO} \approx \lambda$. Therefore, we obtain the condition

$$\frac{W}{\ell_{\rm SO}} \approx \frac{\Delta_{\rm SO}}{\Delta}, \tag{S8}$$

which expresses the ideal geometry as a function of the continuum parameters only.

Let us exemplify the practical use of this relation. In the main text, we assumed a superconducting gap of $\Delta = 1\,\mathrm{meV}$, which is appropriate for e.g. Nb and Pb [2]. Let us now take $\Delta = 0.5\,\mathrm{meV}$, which is appropriate for e.g. Sn and V [2]. Using the relation Eq. (S8) above, we simulate a larger system compared to that of Fig. 3b, with $W_{\rm SC} = 100\,\mathrm{nm}$, $W_{\rm N} = 100\,\mathrm{nm}$. Fig. S2 shows the resulting topological phase diagram, which indeed exhibits topological regions with a topological gap comparable to $\Delta_{\rm SO}$, but the topological region is smaller, indicating that further optimization might be necessary.

BOUNDS ON THE TOPOLOGICAL GAP

Here we discuss the bounds limiting the topological gap, in order to justify the choice of comparing it to $\Delta_{\rm SO}$, which we made in Fig. 3b of the main text.

To set the stage, we study the topological nanowire model [3, 4]

$$H = \left(\frac{k^2}{2m^*} + uk\sigma_z - \mu\right)\tau_z - B\sigma_x + \Delta\tau_x, \tag{S9}$$

where B is the applied Zeeman field and u is the SOC parameter. For simplicity, we focus on $\mu = 0$ where the condition for a topological phase is $B > \Delta$. The two relevant energy scales are Δ and $\Delta_{\rm SO} = mu^2/2$, and the question is whether or not they both set a bound on the energy gap in the topological phase.

At finite B and Δ there are two minima of the gap in the spectrum as a function of the momentum k, one at $k = 0$ and the other near the Fermi momentum. The topological gap of the system is determined by the smallest of the two, when $B > \Delta$. It is maximized at $B = B^* > \Delta$, for which the gap at $k = 0$ is equal to the gap near the Fermi momentum. A closed-form expression for B^* is hard to obtain, but it is straightforward to find it numerically given the values of the other parameters.

Fig. S3(a) shows the maximal topological gap as a function of $\Delta/\Delta_{\rm SO}$, normalized by Δ and by $\Delta_{\rm SO}$. For InAs/InSb nanowires proximitized by Al, Δ and $\Delta_{\rm SO}$ are of the same order of magnitude. However, for a InAs/InSb 2DEG such as the one we studied, $\Delta \gg \Delta_{\rm SO}$ and therefore we analyze the asymptotic behavior of the maximal topological gap in this limit—see the dashed lines in Fig. S3(a). By fitting the asymptotes, which can be obtained numerically or analytically, we find that the maximal topological gap in this limit is $\sim \sqrt{2\Delta_{\rm SO}\Delta}$. Therefore, the gap can be parametrically larger than $\Delta_{\rm SO}$. However, it is evident and also seen in Fig. S3(a) that the gap cannot exceed Δ.

The situation is qualitatively different for the quantum-well model studied here, see Eq. (4) and Fig. 3. We demonstrate this by using the same parameters as in Fig. 3b, with the phases optimally chosen, and vary the ratio $\Delta/\Delta_{\rm SO}$. The results are shown in Fig. S3(b). It is clear from this figure that for our system, the maximal gap in the topological region is of order $\Delta_{\rm SO}$ (at the optimal configuration), but it is much smaller than Δ.

STABILITY TO PERTURBATIONS

In this section, we analyze the stability of the topological phase in the quantum-well model to perturbations in the model's parameters. We demonstrate the robustness of the topological gap to various realistic imperfections, which makes our proposal favorable for experiments.

The parameters used in Fig. S4 are the same as those of Fig. 3b of the main text, with $\theta = 0.55\pi$, $\phi = 0.88\pi$, a representative point inside the topological region. On top of these, we add perturbations as listed below. We plot the topological invariant $\mathcal{Q}$ multiplied by the energy

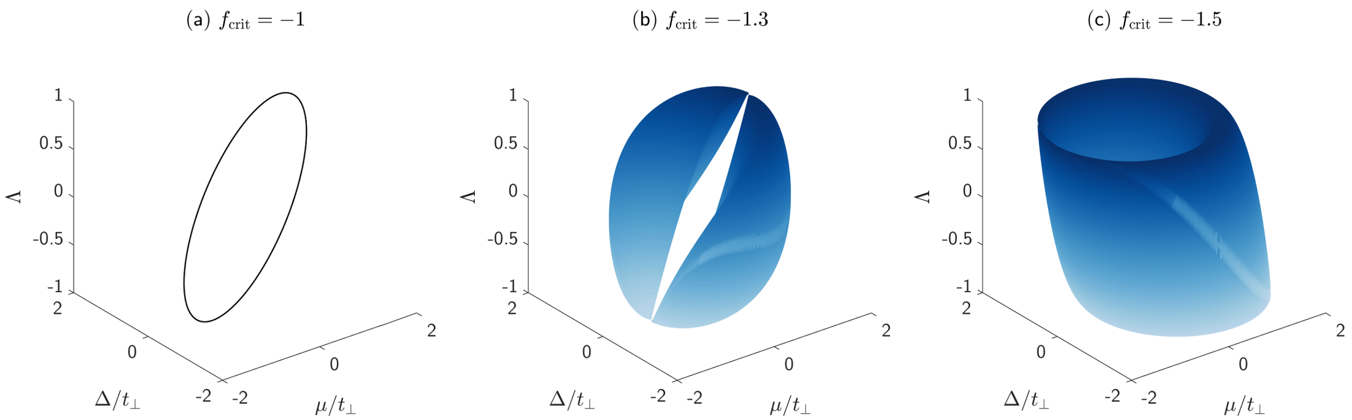

FIG. S1. Critical manifold, marking the topological phase boundaries, in $\mu/t_\perp$, $\Delta/t_\perp$, Λ space for (a) $f_{\rm crit}=-1$, (b) $f_{\rm crit}=-1.1$, (c) $f_{\rm crit}=-1.5$, determined by the solution given in Eq. (S5). As $f_{\rm crit}$ becomes more negative, the manifold's area increases. For a given value of $f_{\rm crit}$, the system is topological at all points contained in the volume surrounded by the surface. For $f_{\rm crit}=-1$ the manifold shrinks into a circle, as seen from Eq. (S7). Alternatively, fixing a point in the parameter space, we can contain it within the volume surrounded by the surface by changing f, leading to a topological state.

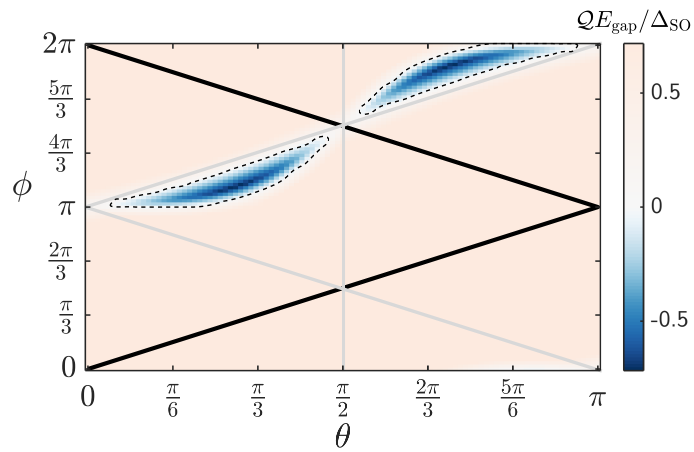

FIG. S2. Topological phase diagram of the quantum-well model, same as in Fig. 3b, with $\Delta=0.5\,$meV and $W_{\rm SC}=100\,$nm, $W_{\rm N}=100\,$nm, $\mu=109.5\,$meV, $t_\perp=0.28\,$meV.

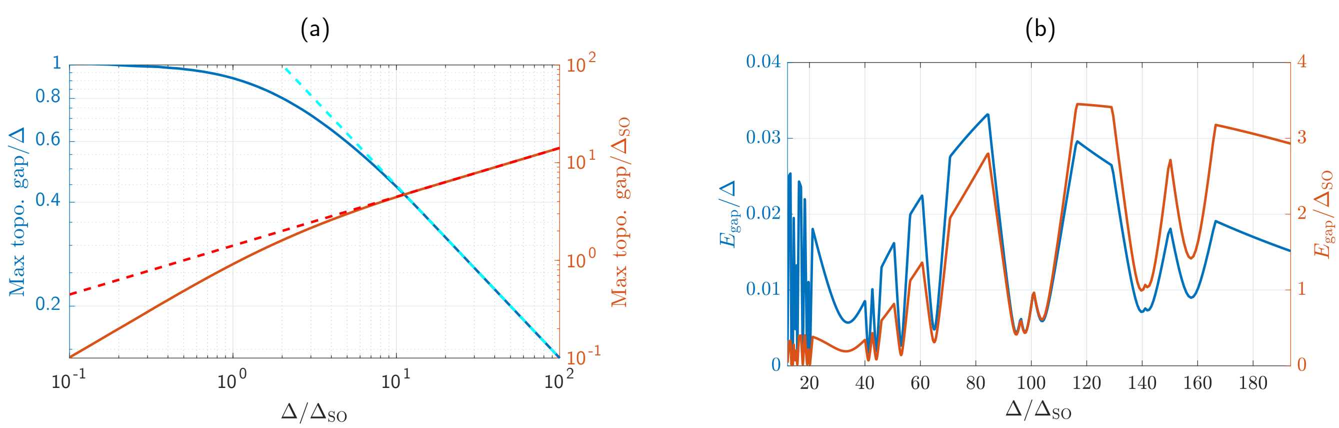

FIG. S3. (a) Maximal topological gap for the nanowire model Eq. (S9) (see also Refs. [3, 4]), as a function of $\Delta/\Delta_{\rm SO}$. The topological gap is normalized by Δ (blue) and by $\Delta_{\rm SO}$ (orange), and plotted in a log-log scale. The dashed lines are the asymptotic forms at $\Delta\gg\Delta_{\rm SO}$, which is $\sqrt{2\Delta_{\rm SO}\Delta}$, i.e., the topological gap may be parametrically larger than $\Delta_{\rm SO}$. (b) Same for the quantum-well model Eq. (4), using the same parameters of Fig. 3b. The maximal topological gap is of order $\Delta_{\rm SO}$, and since $\Delta\gg\Delta_{\rm SO}$ for the parameters we used, it is much smaller than Δ.

gap, *without* even changing the SC phases at all (which is probably the simplest experimental knob).

In Fig. S4(a), the perturbation is a variation in the inter-layer hopping amplitude $t_\perp$. In Fig. S4(b), the chemical potential in the two layers is different: $\mu_{\text{top}} = \mu + \delta\mu$, $\mu_{\text{bottom}} = \mu - \delta\mu$. In Fig. S4(c), the pair potential in the two layers is different: in the main text we took $\Delta_{\text{top}} = \Delta$, $\Delta_{\text{bottom}} = 0$, and now we take $\Delta_{\text{top}} = \Delta + \delta\Delta$, $\Delta_{\text{bottom}} = -\delta\Delta$. Finally, in Fig. S4(d) we add an inter-layer pair potential $\Delta_{\text{inter}}\tau_x\rho_x$.

Under all these perturbations, the topological phase is robust in an appreciable range of parameters. The important implication of this finding is that no fine-tuning is required to drive the system into the topological phase. We stress again that these reassuring results are obtained without further tuning of the SC phases, which will likely increase the stability even more.

* omri.lesser@weizmann.ac.il

[1] B. van Heck, S. Mi, and A. R. Akhmerov, Physical Review B **90**, 155450 (2014).

[2] B. T. Matthias, T. H. Geballe, and V. B. Compton, Reviews of Modern Physics **35**, 1 (1963).

[3] R. M. Lutchyn, J. D. Sau, and S. Das Sarma, Physical Review Letters **105**, 077001 (2010).

[4] Y. Oreg, G. Refael, and F. von Oppen, Physical Review Letters **105**, 177002 (2010).

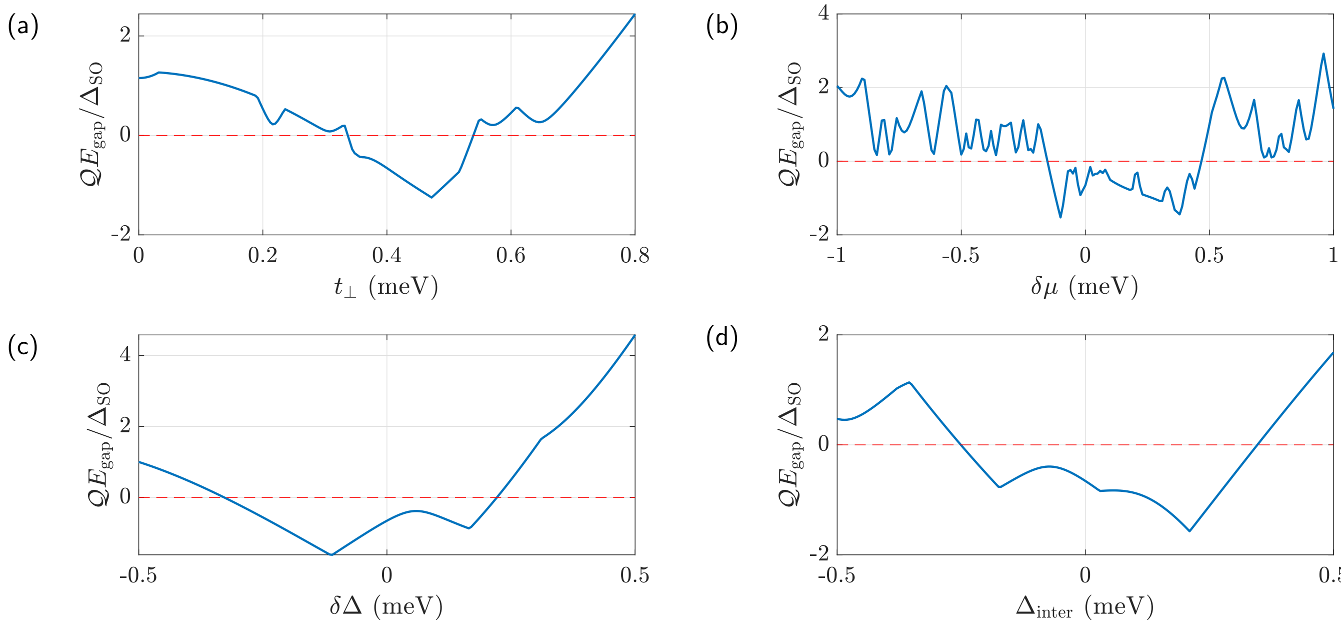

FIG. S4. Stability of the topological phase in the quantum-well model to perturbations in (a) the inter-layer hopping $t_\perp$, (b) a difference $\delta\mu$ in the chemical potential between the two layers, (c) a difference $\delta\Delta$ in the pair potential between the two layers, and (d) inter-layer pair potential Δ_{inter}. Plotted is the topological invariant $\mathcal{Q}$ multiplied by the energy gap in units of the SOC energy. The dashed red line marks the topological phase boundaries.